FEBS 19155 FEBS Letters 415 (1997) 33–39

Laminin α2 chain-null mutant mice by targeted disruption of the *Lama2* gene: a new model of merosin (laminin 2)-deficient congenital muscular dystrophy

Yuko Miyagoe[a,d], Kazunori Hanaoka[b], Ikuya Nonaka[c], Michiko Hayasaka[b], Yoko Nabeshima[d,e], Kiichi Arahata[a], Yo-ichi Nabeshima[d,e], Shin'ichi Takeda[d,*]

[a]*Department of Neuromuscular Research, National Institute of Neuroscience, National Center of Neurology and Psychiatry, 4-1-1 Ogawa-higashi, Kodaira, Tokyo 187, Japan*
[b]*Department of Biosciences, School of Science, Kitasato University, 1-15-1 Kitasato, Sagamihara, Kanagawa 228, Japan*
[c]*Department of Ultrastructural Research, National Institute of Neuroscience, National Center of Neurology and Psychiatry, 4-1-1 Ogawa-higashi, Kodaira, Tokyo 187, Japan*
[d]*Department of Molecular Genetics, National Institute of Neuroscience, National Center of Neurology and Psychiatry, 4-1-1 Ogawa-higashi, Kodaira, Tokyo 187, Japan*
[e]*Institute for Molecular and Cellular Biology, Osaka University, 1-3 Yamada-oka, Suita, Osaka 565, Japan*

Received 4 July 1997; revised version received 29 July 1997

Abstract **Using the gene targeting technique, we have generated a new mouse model of congenital muscular dystrophy (CMD), a null mutant for the laminin α2 chain. These homozygous mice, designated dy^{3K}/dy^{3K}, are characterized by growth retardation and severe muscular dystrophic symptoms and die by 5 weeks of age. Light microscopy revealed that muscle fiber degeneration in these mice begins no later than postnatal day 9. In degenerating muscles, considerable amounts of TUNEL positive nuclei were detected as well as DNA laddering, suggesting increased apoptotic cell death was involved in the process of muscle fiber degeneration.**

Key words: Laminin α2 chain; Gene targeting; Skeletal muscle; Basal lamina; Apoptosis; Muscular dystrophy

1. Introduction

The laminin α2 chain is a tissue-restricted heavy chain component of laminin, a basement membrane-associated molecule expressed mainly in striated muscle, Schwann cells, and trophoblast [1,2]. Specific mutations in the gene that encodes the laminin α2 chain cause a merosin (laminin 2)-deficient congenital muscular dystrophy (CMD) [3], and autosomal recessive muscle disorder. Researchers have identified two animal models of this disease, *dy/dy* [4–7] and dy^{2J}/dy^{2J} [8,9] mice. These models have provided valuable information about the importance of laminin α2 chain in CMD, but are limited because they permit the expression of the chain, either in a greatly reduced or in a truncated form. This paper explains the use of homologous recombination to generate a new CMD mouse model, a null mutant for the laminin α2 chain.

2. Materials and methods

2.1. Embryonic stem (ES) cell selection

A 5.4 kbp mouse genomic DNA fragment containing a portion of the *Lama2* gene was isolated from a 129/Sv mouse genomic library (Stratagene) and subcloned into Bluescript II SK$^+$ vector (Stratagene). A pMC1neo polyA$^+$ cassette (Stratagene) was then inserted into an exon (385–627, +1 denotes the translation start site, amino acids 128–209) [10] followed by the insertion of the MC1TK gene into the 3′-end of the genomic fragment as shown in Fig. 1a. This targeting vector was linearized by cleaving it at its unique *Not*I site, then electroporated into E14 ES cells [11]. Positive clones were selected by challenging the ES cultures with G418 (0.3 mg/ml) and gancyclovir (2 μM) as previously described [11] and, subsequently, screening the surviving cultures using PCR (primer 1 (*Lama2* intron sequence): 5′-CTT TCA GAT TGC ATT GCA AGC-3′, primer 2 (*neo* cassette sequence): 5′-TCG TTT GTT CGG ATC CGT CG-3′). The results of the PCR reactions were confirmed by a Southern blot using the probe shown in Fig. 1a. The injection of positive ES clones into blastocysts was also carried out as already described [11].

2.2. Indirect immunofluorescence

Rat monoclonal antibodies against the mouse laminin α2 chain, 4H8-2 [12], and against the mouse laminin α1 chain, 198 [13], were provided by Dr. L. Sorokin. A rat monoclonal antibody against laminin γ1 (B2) chain was obtained from Chemicon Int. Inc. (Temecula, CA). Cryostat was used to prepare 6–8 μm cryosections for hematoxylin-eosin staining or indirect immunofluorescence. After incubation with primary antibodies (1:10 dilution for monoclonal antibodies), the sections were washed in PBS, then incubated with rhodamine-labeled secondary antibodies (1:200 dilution, Organon Teknika Corp., Durham, NC) to reveal the primary antibodies.

2.3. Western blot

Muscle cryosections were boiled for 5 min in a buffer containing 15% sodium dodecyl sulfate (SDS), 70 mM Tris-HCl (pH 6.7), 10 mM EDTA, and 5% β-mercaptoethanol. After centrifugation, the protein content of the supernatants was estimated using the BioRad protein assay system. The muscle extracts were then separated on a 6% SDS-polyacrylamide gel, and electrotransferred to Immobilon membranes (Millipore). 2D9 [14] was used at a 1:10 dilution. Antibody binding was revealed by horseradish peroxidase-linked sheep anti-mouse Ig and the enhanced chemiluminescence method (Amersham).

2.4. Transmission electron microscopy

Specimens of anterior tibial muscles from 11-day-old wild-type and dy^{3K}/dy^{3K} mice were fixed in 2.5% glutaraldehyde, rinsed in 0.1 M cacodylate buffer (pH 7.2), postfixed in 1% OsO_4 in cacodylate buffer, then embedded in resin. Ultrathin sections were stained with uranyl acetate and lead citrate, then examined with a Hitachi H-600 electron microscope.

2.5. DNA laddering assays

Genomic DNA was extracted from calf muscles using lysis buffer (150 μg/ml proteinase K, 1 mg/ml pronase E, 50 mM Tris-HCl pH 8.0, 0.1 M NaCl, 20 mM EDTA and 1% SDS). After treatment with RNase, 5 μg of genomic DNA was labeled with [α-^{32}P]dCTP using terminal transferase [15] (Boehringer Mannheim), resolved on a 2.0%

*Corresponding author. Fax: (81) (423) 46-3864.
E-mail: takeda@ncnaxp.ncnp.go.jp

PII S0014-5793(97)01007-7

agarose gel, transferred to a nylon membrane (Hybond-N$^+$, Amersham), and, finally, visualized using autoradiography.

2.6. TUNEL (terminal deoxynucleotidyl transferase-mediated dUTP nick end-labeling) technique [16]

Cryosections of calf muscles (10 μm) were fixed with 10% neutral buffered formalin for 10 min at room temperature. The sections were then post-fixed in ethanol:acetic acid (2:1) for 5 min at −20°C, labeled with DIG-conjugated dUTP, reacted with a peroxidase-conjugated anti-DIG antibody (Oncor), and then stained with amino-9-ethylcarbazole as substrate to produce a red reaction product (Zymed), and counterstained with methyl green. The numbers of TUNEL positive nuclei were counted on photographs of 10–20 different sections. With a stage micrometer, we estimated the average number of TUNEL positive nuclei (nuclei/mm^3) in each sample.

3. Results and discussion

To construct a gene-targeting vector for disruption of the mouse laminin α2 chain (*Lama2*) gene, a genomic fragment that includes an exon which encodes a part of domain VI of the laminin α2 chain [10] was subcloned into the Bluescript II SK$^+$ vector. A neomycin resistance cassette (*neo*) was then inserted into the exon in reverse orientation (Fig. 1a). For negative selection, the HSV thymidine kinase (*tk*) gene was ligated to the new construct. The resulting vector was linearized and transfected into ES cells (E14) by electroporation. Gancyclovir-G418 doubly resistant colonies were then selected as already described [11]. The homologous recombination was first identified by PCR, then confirmed by Southern blotting (data not shown). Four independent ES clones were injected into C57BL/6 blastocysts to obtain germ line chimeras [11]. The male chimeric mice were then allowed to breed with female ICR, BALB/c and 129/Sv mice resulting in the transmission of the mutated alleles of two independent ES clones to the offspring. The presence of the targeted allele in the offspring was detected by Southern blot analysis (Fig. 1a,b). Heterozygotes were phenotypically normal and were used to breed homozygous mice. The homozygotes appeared at the frequency predicted according to Mendelian genetics. Newborn homozygous mice were indistinguishable from their heterozygous or wild-type littermates at birth, while by postnatal

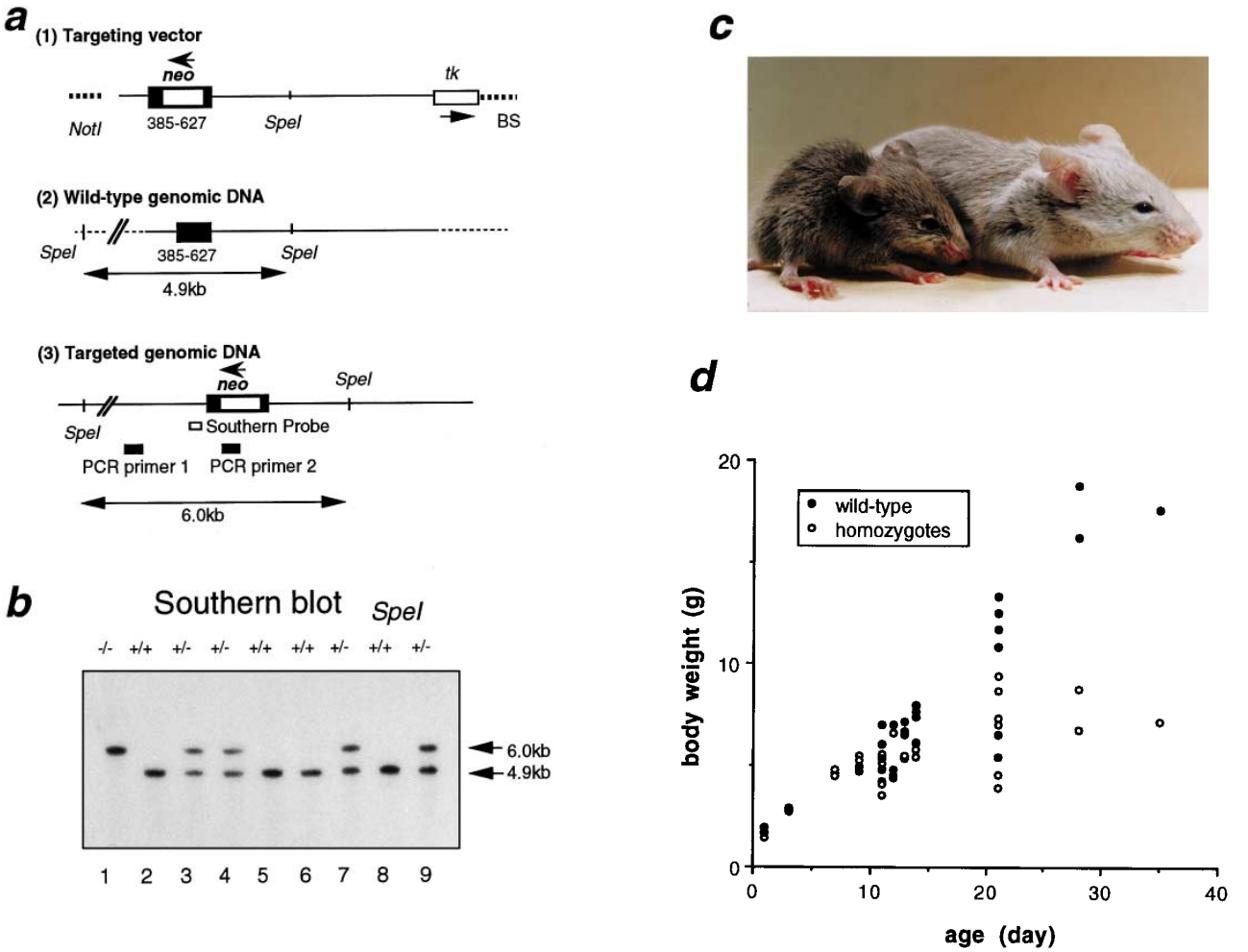

Fig. 1. Generation of the laminin α2 chain (*Lama2*) gene targeted mice using homologous recombination. a: Strategy of the targeted disruption of the *Lama2* gene in ES cells. b: Southern blot of genomic DNA isolated from each pup of a litter born to heterozygous (+/−) parents. Genomic DNA (10 μg) was digested with *Spe*I and hybridized with the DNA probe illustrated in a part of a. The wild-type and targeted loci generate 4.9 kb and 6.0 kb *Spe*I fragments, respectively. A homozygote (−/−) is shown in lane 1. Heterozygotes' DNA (+/−) are in lanes 3, 4, 7 and 9, and their wild-type littermates' (+/+) are in lanes 2, 5, 6 and 8. c: Photograph of wild-type (right) and mutant (left) littermates on postnatal day 28 (P28). d: Growth of mutant mice and their wild-type littermates. The body weight of wild-type (34 mice) and homozygous mutant mice (31 mice) is plotted. Heterozygotes grow at the same rate as their wild-type littermates.

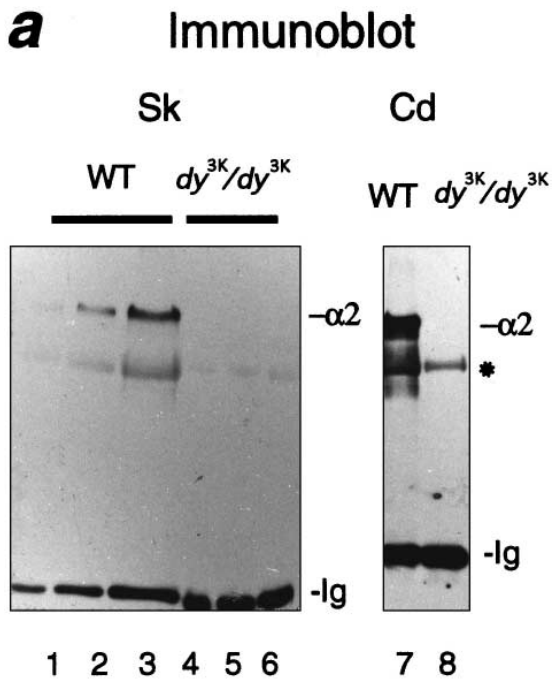

Fig. 2. The *Lama2* gene targeted mice are null mutants. a: Western blot using a monoclonal antibody against the laminin α2 chain, 2D9 [14]. Extraction lysates from wild-type calf muscles (WT) are loaded in lanes 1–3, and samples from dy^{3K}/dy^{3K} muscle are in lanes 4–6. The amount of protein used is: 5 μg in lanes 1 and 4, 10 μg in lanes 2 and 5, and 20 μg in lanes 3 and 6. Extracts from cardiac muscle were also analyzed (lanes 7, 8). The asterisk indicates a non-specific band. b: No laminin α2 chain immunopositive fibers in mutant calf and cardiac muscles. Acetone-fixed frozen sections of wild-type (WT) and dy^{3K}/dy^{3K} calf muscles were stained with a rat monoclonal antibody, 4H8-2 [12], against the mouse laminin α2 chain.
←

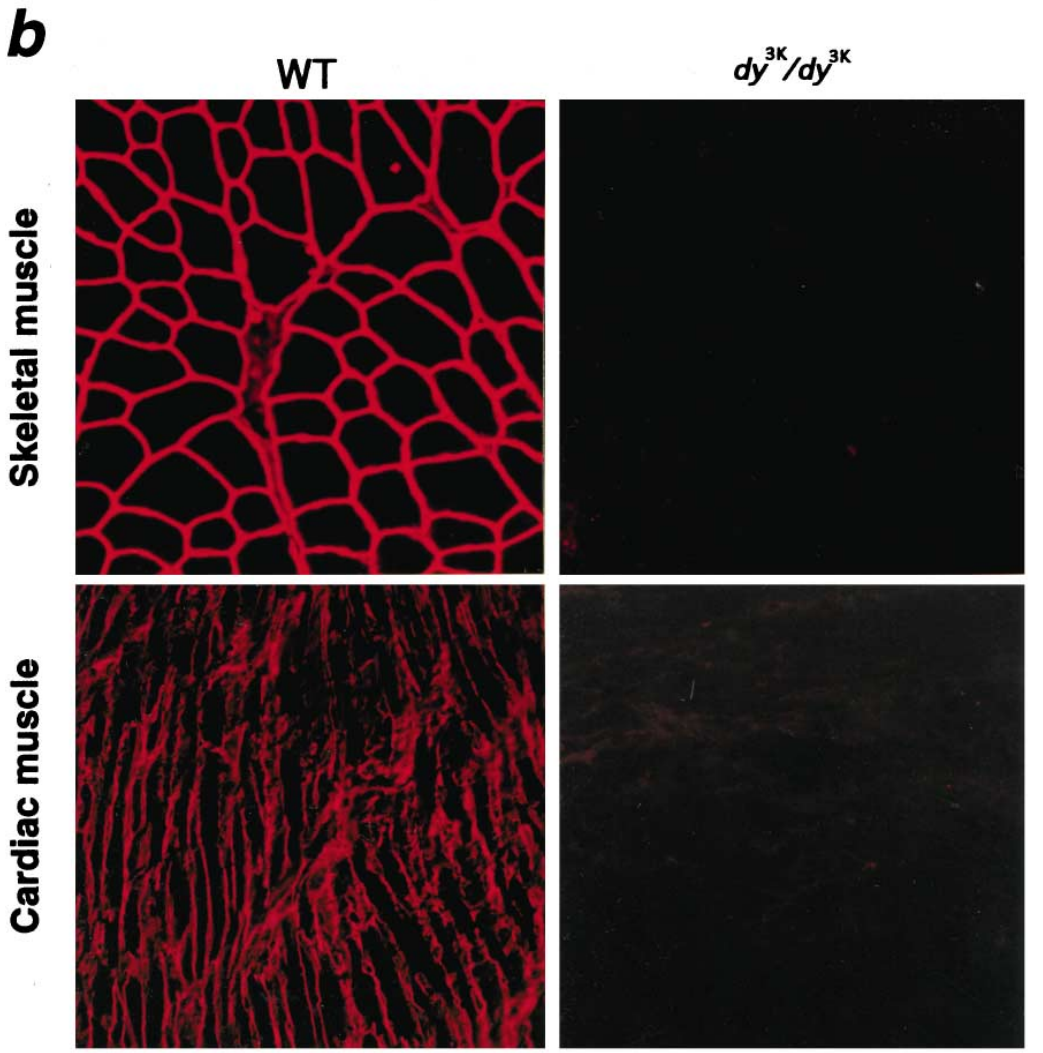

day 14 (P14), their retarded growth became apparent; from this point, their body size remained comparatively small for the remainder of their lives (Fig. 1c,d). By P21, these mice displayed overt dystrophic symptoms, such as waddling gait and twitching, characteristic of *dy/dy* dystrophic mice [4]. However, unlike previously studied dystrophic mice, these mice succumbed to undetermined causes by 5 weeks of age. In comparison, the average life span of *dy/dy* mice has been reported to be 5–6 months [17].

Immunoblotting with the mouse anti-laminin α2 chain monoclonal antibody, 2D9 [14], which binds the G2–G3 region of the G domain, failed to detect either the 300 kDa C-terminal fragment or truncated laminin α2 chain in homozygous skeletal or cardiac muscle (Fig. 2a). Indirect immunostaining with the rat monoclonal antibody, 4H8-2 [12], which also recognizes the 300 kDa portion of the protein, confirmed the absence of the laminin α2 chain in both muscles (Fig. 2b). Dystrophic *dy/dy* mice [4], carrying an unidentified mutation in the *Lama2* gene [5–7], express low but detectable levels of the laminin α2 chain while dy^{2J}/dy^{2J} mice express a truncated form of the chain [8,9]. The homozygous mice described in this paper are null mutants and they have been designated dy^{3K}/dy^{3K}. Since there are no significant differences in phenotypic expression in dy^{3K}/dy^{3K} mice that have different genetic backgrounds, the results reported here are limited to mice of the ICR background.

Before P9, dy^{3K}/dy^{3K} skeletal muscles are comparable to those of their wild-type littermates when examined using hematoxylin-eosin staining. Scattered degenerative fibers began to appear at P9 (see Fig. 3a), and, at P11, numerous degenerated muscle fibers along with extensive infiltrates and evidence of phagocytosis could been seen (see Fig. 3a). At P13, groups of centrally nucleated small-caliber muscle fibers appeared, revealing the process of active regeneration (see Fig. 3a). The changes in skeletal muscle progressed focally, rather than diffusely, and were more prominent in calf muscles than in thigh muscles. In spite of active regeneration in the early neonatal stage, degeneration continued and resulted in the variability of fiber size and proliferation of endomysial connective tissue observed at P21 and P28 (not shown).

To determine the molecular basis of the muscle fiber degeneration, we analyzed the influence of laminin α2 chain depletion on the basal lamina of skeletal muscle. The laminin γ1 chain (Fig. 3b), collagen type IV and perlecan (not shown), other constituents of basal lamina, were clearly immunostained around the muscle fibers of 4 week old dy^{3K}/dy^{3K} mice, although the staining was more sparse than that of their wild-type littermates. The same results were obtained using P3 and P13 mutant muscle (not shown). Laminin α1, which localizes at the neuromuscular junctions of normal muscle, was slightly up-regulated in dy^{3K}/dy^{3K} mutant muscles, when immunostained with a rat monoclonal antibody, 198 [13] (see Fig. 3b). Dystrophin, a muscle-specific membrane-related cytoskeletal protein, was expressed at an equivalent level in both control and mutant muscles (not shown). At the neuromuscular junction, neuronal cell adhesion molecule and the dystrophin-related protein, utrophin, stained normal proportions (data not shown). Although it seemed that most constituents of the basal lamina were present, there was a nearly complete absence of the basal lamina around the muscle fiber and around the Schwann cells of peripheral nerves in electron microscopic examination (Fig. 4). This defect in the basal lamina was also discovered in *dy/dy* [5,6] mice but was thinner and discontinuous.

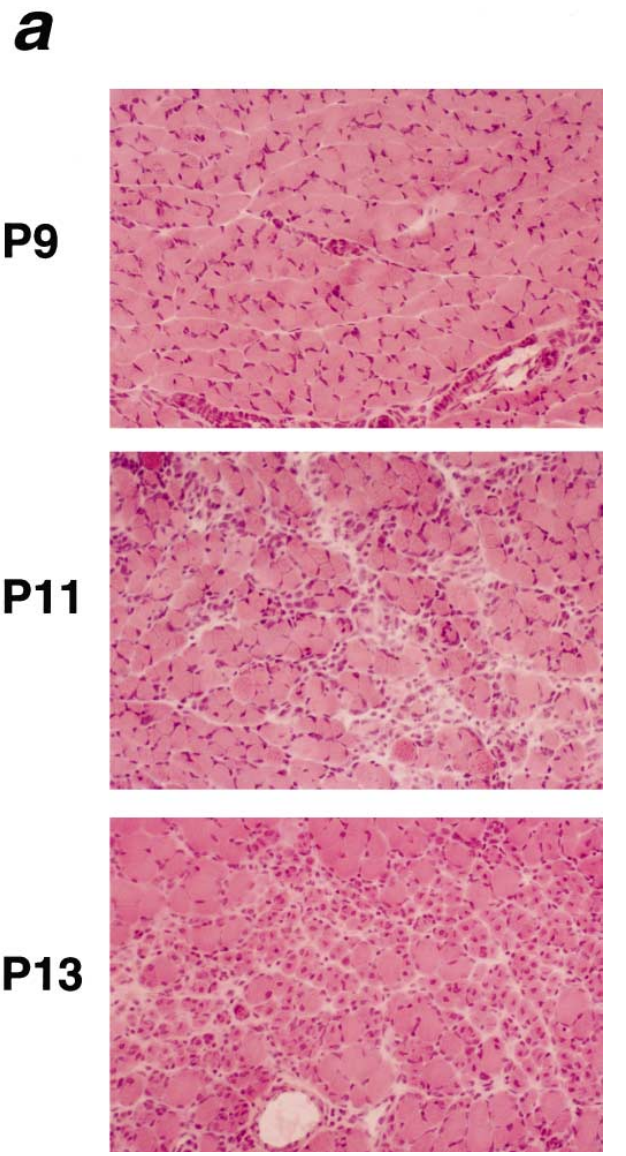

Fig. 3. In mutant mice, muscle degeneration appeared at an early neonatal period. a: Muscle fiber degeneration and regeneration occurred in the calf muscles of mutant mice. These are representative sections from postnatal day 9 (P9), P11 and P13. Hematoxylin-eosin staining, ×200. b: Cryosections of skeletal muscles from 3 week old mice were stained with rat monoclonal antibodies against the laminin α1 chain, 198 [13], and the laminin γ1 chain (Chemicon). Magnification: ×400.

→

Recently, it was reported that the lack of the laminin α2 chain results in apoptotic cell death in myogenic cells in vitro, where the laminin α2 chain appears to promote myotube stability by preventing apoptosis [18]. To determine whether the absence of the laminin α2 chain in dy^{3K}/dy^{3K} mice causes apoptotic muscle cell death, we used TUNEL [16] to search for apoptosis-associated DNA strand breaks in situ (Fig. 5). In the degenerating muscle of dy^{3K}/dy^{3K} mice (P11), there were a markedly higher number of TUNEL positive nuclei, compared to the muscles of their wild-type littermates. The

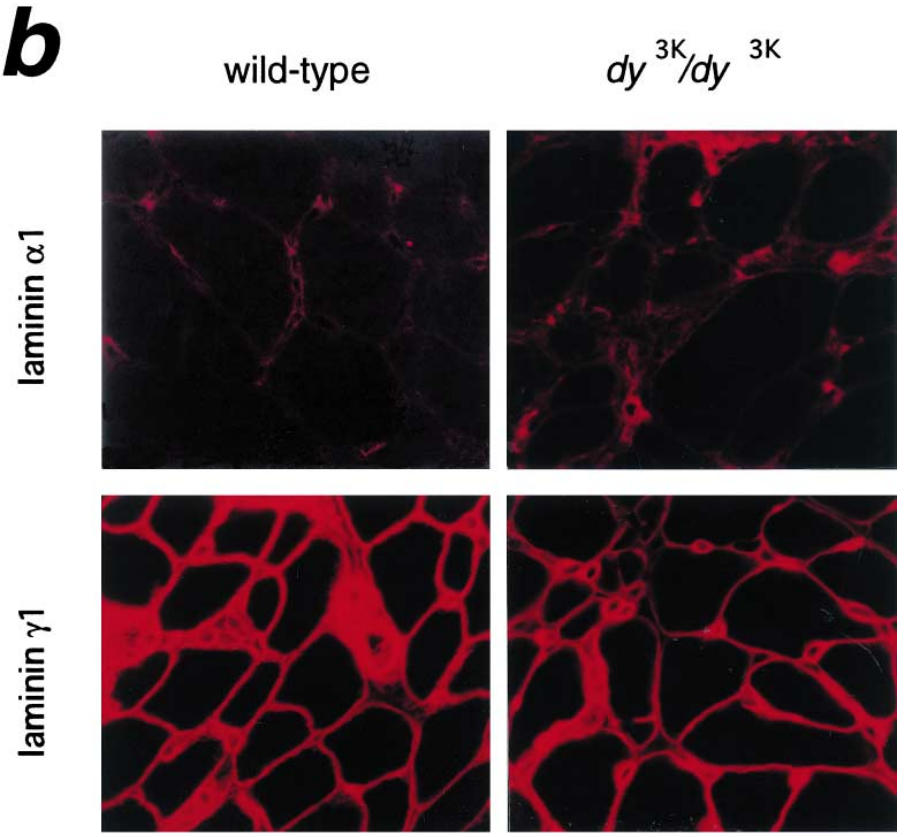

TUNEL positive cells were visible at the surface of muscle fibers that had no apparent degeneration (Fig. 5a) and those existing in areas with extensive infiltrates (Fig. 5a). We then extracted genomic DNA from the affected muscle and carried out DNA laddering assays, using 3′-end labeling with [α-^{32}P]dCTP. Consistent with the TUNEL assay results, genomic DNA from degenerating muscle showed DNA laddering in multiples of about 180 bp, indicating internucleosomal fragmentation (Fig. 5b).

The TUNEL technique was also used to determine the role of apoptosis during dy^{3K}/dy^{3K} muscle development before P11. The number of TUNEL positive nuclei in the muscles of null mutant mice at P3, P7 and P9 was not appreciably different from that in wild-type muscles (Fig. 5c). It is possible that early neonatal mutant muscles contain trophic factors that prevent apoptotic cell death in neonatal myofibers lacking the laminin α2 chain. These effects are less important at P11, when degeneration is most prominent and TUNEL positive nuclei increase to as much as 1% of the total number of nuclei (Fig. 5c). At this time, necrotic changes and inflammatory infiltrates also become apparent. Dystrophic dy^{3K}/dy^{3K} mice experience both apoptotic and necrotic cell death in their degenerating muscles. Recent studies have reported an increase in programmed cell death in dystrophin deficient *mdx* mice [19–22], though the mechanism has not yet been determined. Likewise, the trigger of apoptotic cell death in dy^{3K}/dy^{3K} mutant myofibers is not clear; the role of apoptosis in muscle degeneration remains to be determined.

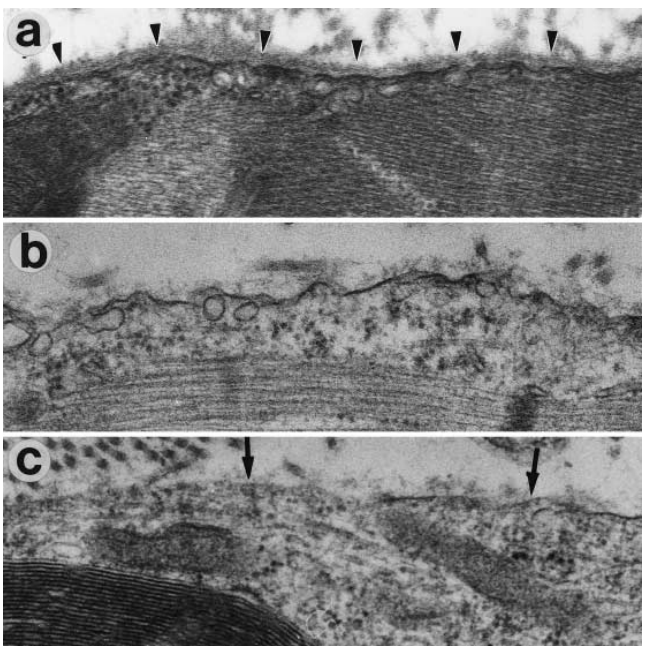

Fig. 4. Transmission electron microscopy of skeletal muscle. The basal lamina, clearly present along the sarcolemma in wild-type mouse (a), was almost completely absent in all muscle fibers of the mutant mouse at P11 (b). The arrowheads point to the basal lamina of muscle fibers. c: The basal lamina of Schwann cells in intramuscular nerve bundles was also absent (indicated by arrows). Magnification: ×50 000.

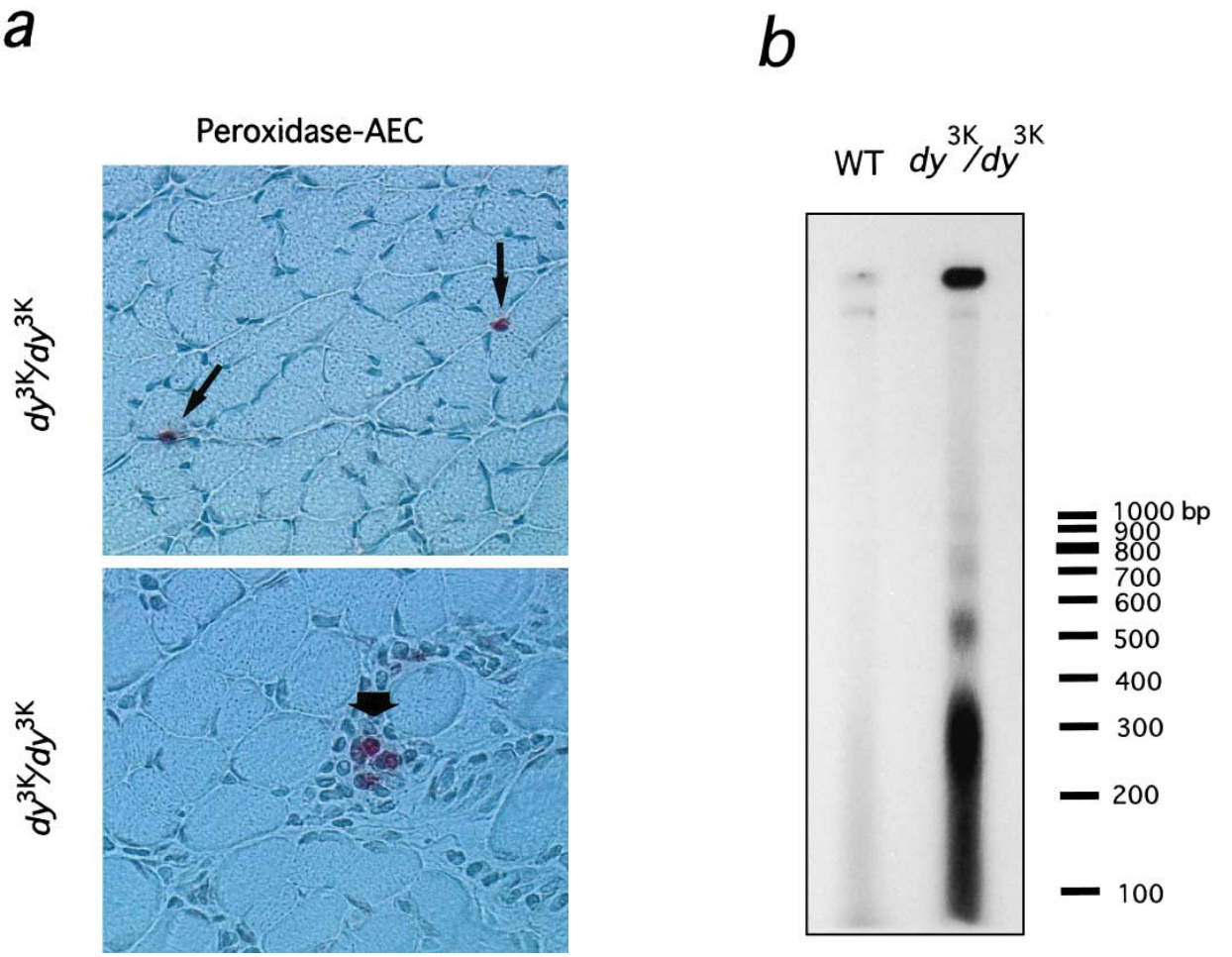

Fig. 5. Detection of apoptosis-associated DNA strand breaks in mutant skeletal muscles. a: In situ detection of DNA fragmentation in mutant (dy^{3K}/dy^{3K}) muscles at P11, using the TUNEL technique [16]. Apoptotic nuclei (arrows) in P11 mutant muscle were labelled with a peroxidase-conjugated anti-DIG antibody using 3-amino-9-ethylcarbazole (red). Magnification: ×400. b: DNA laddering assays of genomic DNA (5 μg/lane) from wild-type (lane 1) and mutant (lane 2) muscles. The migration positions of a 100 bp DNA ladder are indicated. c: Density of TdT-dUTP labeled apoptotic myonuclei in mutant and wild-type muscles of different ages. The estimated average densities (nuclei/mm^3) were plotted with standard error bars.

Laminin α2 chain mRNA [10,23] and protein are expressed in several organs other than striated muscles, including the central nervous system [24], thyroid gland, thymus [25], kidney, testis, skin [26] and digestive tract [27]. Since dy^{3K}/dy^{3K} mice have no laminin α2 chain, they provide an excellent model to analyze the biological functions of laminin α2 chain in these organs.

Acknowledgements: We thank H. Hori for 2D9, and L.M. Sorokin for 198 and 4H8-2. D. Kitamura and T. Watanabe graciously provided E14 cells, and H. Sugita, S. Ebashi, and D. North gave valuable discussion regarding this work. We especially thank K. Kobayashi for excellent technical assistance. This work was supported by research grants for Nervous and Mental Disorders from the Ministry of Health and Welfare, and the Ministry of Education, Science, Sports and Culture, Japan.

References

[1] Leivo, I. and Engvall, E. (1988) Proc. Natl. Acad. Sci. USA 85, 1544–1548.

[2] Ehrig, K., Leivo, I., Argraves, W.S., Ruoslahti, E. and Engvall, E. (1990) Proc. Natl. Acad. Sci. USA 87, 3264–3268.
[3] Tomé, F.M.S., Evangelista, A., Leclerc, A., Sunada, Y., Manole, E., Estournet, B., Barois, A., Campbell, K. and Fardeau, M. (1994) C.R. Acad. Sci. Paris Sci. Vie/Life sci. 317, 351–357.
[4] Michelson, A.M., Russell, E. and Harman, P.J. (1955) Proc. Natl. Acad. Sci. USA 41, 1079–1084.
[5] Arahata, K., Hayashi, Y., Koga, R., Goto, K., Lee, J.H., Miyagoe, Y., Ishii, H., Tsukahara, T., Takeda, S., Woo, M., Nonaka, I., Matsuzaki, T. and Sugita, H. (1993) Proc. Japan Acad. 69, 259–264.
[6] Xu, H., Christmas, P., Wu, X.-R., Wewer, U.M. and Engvall, E. (1994) Proc. Natl. Acad. Sci. USA 91, 5572–5576.
[7] Sunada, Y., Bernier, S.M., Kozak, C.A., Yamada, Y. and Campbell, K.P. (1994) J. Biol. Chem. 269, 13729–13732.
[8] Xu, H., Wu, X.-R., Wewer, U.M. and Engvall, E. (1994) Nature Genet. 8, 297–301.
[9] Sunada, Y., Bernier, S.M., Utani, A., Yamada, Y. and Campbell, K.P. (1995) Hum. Mol. Genet. 4, 1055–1061.
[10] Bernier, S.M., Utani, A., Sugiyama, S., Doi, T., Polistina, C. and Yamada, Y. (1994) Matrix Biol. 14, 447–455.
[11] Nabeshima, Y., Hanaoka, K., Hayasaka, M., Esumi, E., Li, S., Nonaka, I. and Nabeshima, Y. (1993) Nature 364, 532–535.
[12] Schuler, F. and Sorokin, L.M. (1995) J. Cell Sci. 108, 3795–3805.
[13] Sorokin, L.M., Conzelmann, S., Ekblom, P., Battaglia, C., Aumailley, M. and Timpl, R. (1992) Exp. Cell Res. 201, 137–144.
[14] Hori, H., Kanamori, T., Mizuta, T., Yamaguchi, N., Liu, Y. and Nagai, Y. (1994) J. Biochem. 116, 1212–1219.
[15] Tilly, J.L. and Hseuh, A.J.W. (1995) J. Cell. Physiol. 154, 519–526.
[16] Gavrieli, Y., Sherman, Y. and Ben-Sasson, S.A. (1992) J. Cell Biol. 119, 493–501.
[17] Russell, E.S., Silvers, W.K., Loosli, R., Wolfe, H.G. and Southard, J.L. (1962) Science 135, 1061–1062.
[18] Vachon, P.H., Loechel, F., Xu, H., Wewer, U.M. and Engvall, E. (1996) J. Cell Biol. 134, 1483–1497.
[19] Tidball, J.G., Albrecht, D.E., Locensgard, B.E. and Spencer, M. (1995) J. Cell Sci. 108, 2197–2204.
[20] Smith, J., Fowkes, G. and Schofield, P.N. (1995) Cell Death Differ. 2, 243–251.
[21] Matsuda, R., Nishikawa, A. and Tanaka, H. (1995) J. Biochem. 118, 959–964.
[22] Lockshin, R.A., Knight, R.A. and Melino, G. (1995) Cell Death Differ. 2, 231–232.
[23] Vuolteenaho, R., Nissinen, M., Sainio, K., Byers, R., Eddy, R., Hirvonen, H., Shows, T.B., Sariola, H., Engvall, E. and Tryggvason, K. (1994) J. Cell Biol. 124, 381–394.
[24] Yamada, H., Hori, H., Tanaka, T., Fujita, S., Fukuta-Ohi, H., Hojo, S., Tamura, A., Shimizu, T. and Matsumara, K. (1995) FEBS Lett. 376, 37–40.
[25] Chang, A.C., Wadsworth, S. and Coligan, J.E. (1993) J. Immunol. 151, 1789–1801.
[26] Sewry, C.A., Philpot, J., Sorokin, L.M., Wilson, L.A., Naom, I., Goodwin, F., D'Alessandro, M., Dubowitz, V. and Muntoni, F. (1996) Lancet 347, 582–584.
[27] Simon-Assmann, P., Duclos, B., Orian-Rousseau, V., Arnord, C., Mathelin, C., Engvall, E. and Kedinger, M. (1994) Dev. Dyn. 201, 71–85.